(2)

LASER RADAR SYSTEM DEMONSTRATION

NRL Contract Number
N00014-88-C-2278

SYSTEM REQUIREMENTS REVIEW
SECOND DEMONSTRATION RECEIVER

CDRL A006

3 December 1991

Prepared for

NAVAL RESEARCH LABORATORY
WASHINGTON, D.C.

Prepared By

LASER APPLICATIONS DIVISION
SCIENCE APPLICATIONS INTERNATIONAL CORPORATION
4161 CAMPUS POINT COURT
SAN DIEGO, CA 92121

TABLE OF CONTENTS

LIST OF FIGURES

LIST OF TABLES

Statement A per telecon Doug Collins NRL/3220
Washington, DC 20375-5000

NWW 2/14/92

1.0 INTRODUCTION

A conceptual design is currently being developed for a sensor system which is capable of detecting both large and small targets using a pulsed transmitter and high bandwidth receiver. The mission scenario for the large target requires that it first be detected with a small false alarm rate, and immediately classified with a few additional transmitter pulsed. The sensor must also be capable of detecting small targets with a low false alarm rate. Because a number of naturally occurring objects can cause false alarms, it is believed that the most effective means for mitigating these false alarms is to complete the classification or identification of the small target immediately following detection. This must be accomplished with negligible effect on the overall search rate. In addition to the two principal target categories already mentioned, there is a group of very small targets. It is desirable, but not presently a requirement, that the sensor system be capable of detecting these targets also.

Two conceptual approaches have been developed to meet the foregoing performance requirements of the desired sensor system. Both use short -pulse lasers to illuminate the target. In the first approach a high resolution image is created using a single range gate of reflected or backscattered light. The images have a large number of pixels, with square arrays of the order of 128x128 to 256x256. In the second approach, a more limited array of time-resolved pixels is used to gather three-dimensional data of the region containing the target. In the time-resolved approach, the array sizes are more limited because of the requirement for multiple channels of high-speed electronics. Typical array sizes are of the order 2x2 to as large as 16x16. In the extreme, the time-resolved approach can use a single pixel. As might be expected, each of the above approaches has advantages in some regimes of the mission scenarios for the various targets. For example, identification of a small target can benefit from the high spatial resolution of the first approach and detection of a large target at an unknown range can benefit from the high time resolution of the second approach.

To meet the demanding requirements for this sensor system, SAIC has developed the dual-mode detector concept which incorporates both of the above approaches into a single receiver. The dual-mode receiver may use two separate detectors or a single dual-mode Digicon, which was also developed by SAIC. The dual-mode concept, the Digicon and some of the performance characteristics of the detector are described in Section 2. The present state of the design of the Digicon detector is described in Section 3, including the key components; photocathode, electron focussing and electron detectors for the two modes. A conceptual design for the electronic subsystem for the control of the detector and for processing the detector output signals is summarized in Section 4. In Section 5, we outline two approaches to the optical telescope of the receiver. Finally, in Section 6, we address the packaging of the receiver subsystem into an existing pod and suggest means for saving the space which is required for the additional electronics of the Digicon as compared with the presently used photomultiplier tubes.

2.0 DUAL-MODE DIGICON DETECTOR

2.1 Dual-Mode Detector Concept

The Dual-Mode Imaging LIDAR receiver concept takes advantage of the fact that initial object detection can be made with high Probability of Detection (PD) at relatively low spatial resolution using a high bandwidth detector. Once the object is detected, a more detailed image can be generated using a higher resolution low-bandwidth detector. Specifically, it combines:

a) an N x N high temporal bandwidth, low spatial resolution array for detection with

b) a gated, intensified, high spatial resolution CCD array with a nominal 30 Hz frame-rate for identification.

Typical values for the dimensions of the detection array are N = 1 to 3. The value N = 2 is attractive because of the current availability of 2x2 arrays of avalanche photodiodes which have higher overall gain than the more common silicon diodes. Furthermore, analyses indicate that for detection of the large targets, a 2x2 array gives a 3 dB improvement in signal-to-noise over a single pixel detector. The detection array has a bandwidth of about 100 MHz and spatial pixels of two to three times the dimensions of the target being sought. The dimensions of the CCD

array will typically be of the order of 256x256.

The high bandwidth N X N array, which generates multiple gate slices within the water column with a single laser pulse, achieves initial detection of the submerged object and provides an accurate measurement of the object depth. The object depth information is then used to control the gate timing for the high resolution CCD array. This method allows initial object detection to occur with high laser power utilization efficiency and a low matched filter processing load. False alarm mitigation with full classification capability is achieved using optimal gate timing of the higher resolution intensified CCD. An important feature of this method is that all detection and false alarm mitigation/classification tasks can be accomplished with a single, compact Digicon detector assembly coupled to a large aperture, fixed focal length optical system.

2.2 Digicon Implementation of the Dual-Mode System Concept

The preferred embodiment of the Dual-Mode concept employs an electrostatically focused Digicon tube as shown in Figure 2.1. The dimensions and key parameters of the dual-mode Digicon (DMD) are summarized in Table 2.1. The DMD incorporates the following features:

1) A blue-green sensitive field-enhanced GaAs photocathode with a quantum efficiency of up to 40%.
2) A grid immediately behind the photocathode which generates the photocathode quantum efficiency enhancing field and allows the tube to be gated on in less than 10 nanoseconds. The grid can also be biased to effectively control the tube gain, i.e. sensitivity control. This feature can be important during both the detection and false alarm mitigation/classification stages.
3) An anode which incorporates two detectors within the same tube envelope. The first detector is a thinned, backside bombarded CCD which occupies the space in the center of the anode header. The second detector is a high bandwidth silicon diode or avalanche diode array which occupies an off-axis portion of the anode header space not occupied by the CCD array.

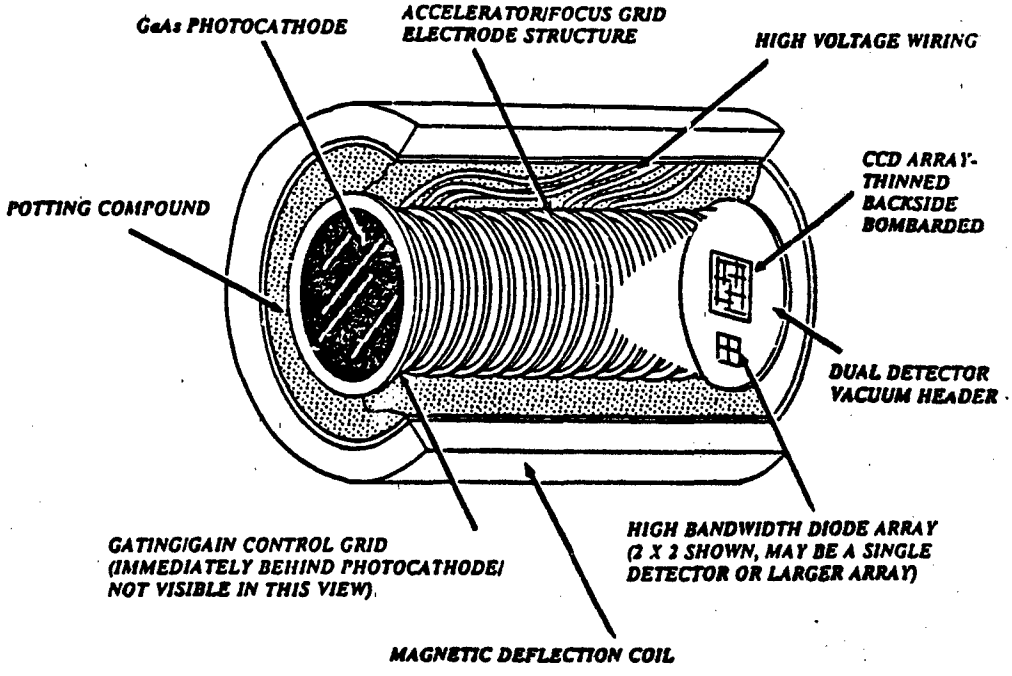

Figure 2.1 Dual-Mode Digicon Detector

Table 2.1 Parameters of Dual-Mode Digicon Detector

PARAMETER	VALUE
TUBE DIAMETER (mm)	25
CCD ARRAY	256 x 256
CCD PIXEL (micron)	20
APD ARRAY	2 x 2
APD PIXEL (mm)	1.5
TUBE VOLTAGE (kV)	15
EBS GAIN	4,166
APD GAIN	100
TOTAL TUBE GAIN	416,600
ELECTRON IMAGE MAGNIFICATIONS	0.25/1.0

4) Both the CCD array and the high bandwidth diode array are operated in the electron bombardment in silicon (EBS) gain mode.

5) A deflection coil surrounding the digicon which allows the electron flux from the photocathode to be deflected to the diode array during detection mode operation. During classification mode operation the deflection coil is in an off state so that the photoelectron image generated by the photocathode can be electrostatically imaged onto the CCD array.

6) Two sets of potentials are applied to the accelerator rings of the Digicon. The first set of potentials is associated with the detection mode of operation when the deflection coil is in an "on" state. For N > 1 these potentials image the photocathode onto the diode array. If a single pixel is used, N=1, then the photocathode is simply mapped onto the single detector without the requirement to preserve photocathode image information. The second set of potentials is associated with the classification mode of operation when the deflection coil is in an "off" state. These potentials image the photocathode onto the CCD in the center of the anode header.

7) The two sets of potentials applied to the accelerator rings of the Digicon can be adjusted to provide a zoom electron image magnification capability. This allows the effective pixel size on the photocathode to be adjusted over a range on the order of 4-to-1.

8) The CCD incorporated in the center of the vacuum header has the ability to perform pixel binning to increase the effective pixel size. For example, with 20 micron pixel sites on the CCD, 4 x 4 binning will result in an effective pixel size of 80 microns.

The small pixel sizes associated with CCD arrays normally dictates that the receiver optics have a relatively short focal length to produce the large pixel sizes desired for the classification of large objects. Even with short focal length receiver optics, some CCD pixel binning may required. To maintain the required image resolution over a wide instantaneous field of view, the

receiver F-number must be no lower than about 1.0. This implies that the receiver aperture size is severely limited, thereby limiting light-gathering power and, consequently, the signal-to-noise ratio (SNR) of the image. Furthermore, to generate the desired wide range of pixel sizes with the conventional gated intensified CCD array, a zoom capability must be incorporated in the receiver optics, placing further constraints on the maximum receiver aperture size. The capabilities of the Dual-Mode Imaging LIDAR receiver described in items 7) and 8) substantially remove the foregoing constraints. When CCD pixel binning is combined with electrostatic zoom magnification capability in the Digicon tube, the full range of desired pixel sizes can be generated with a fixed focal length receiver optical system. Furthermore, the focal length of the optical system can be considerably longer, leading to an increase in the aperture size for an F-1 optical system.

In Section 5, two concepts for the optical telescope are reviewed for the receiver; a hybrid telescope based on the Gabor-Cassegrain and an improved version of the afocal refractive telescope designed by Sanders. The effective array sizes and pixel dimensions in the target and focal planes for the two telescopes and the dual-mode Digicon are summarized in Table 2.2.

Table 2.2 Pixel Parameters for Dual-Mode Digicon Receiver

TARGET SIZE	EFFECTIVE PIX ARRAY	TARGET PLANE PIX/SPOT (m)	FOCAL PLANE PIXEL/SPOT (mm)		TUBE MAG	BINS	EFFECTIVE ANODE PIXEL
			GABOR-CASSEGRAIN	IMPROVED AFOCAL+ 80 mm 645			
DETECTION MODE							
LARGE	2 X 2	20 / 40	8.9 / 17.8	8 / 16	0.25	1	2.23 mm
SMALL	2 X 2	5 / 10	2.2 / 4.45	2 / 4	1.0	1	2.23 mm
VERY SMALL	64 X 64	0.156 / 10	0.069 / 4.45	0.062 / 4	1.0	4	0.062 mm
IDENTIFICATION MODE							
LARGE	32 X 32	1.25 / 40	0.556 / 17.8	0.5 / 16	0.25	8	0.125 mm
SMALL	64 X 64	0.156 / 10	0.069 / 4.45	0.0625 / 4	1.0	4	0.062 mm
VERY SMALL	256 X 256	0.04 / 10	0.0174 / 4.45	0.0156 / 4	1.0	1	15.6 μm

2.3 Dual-Mode System Operation

Three separate phases of operation can be identified for the Dual-Mode Imaging LIDAR system:

I. **Surface Flash Detection.** In this phase the photocathode gating grid can be biased to produce low tube gain. The deflection coil is activated to deflect the electron image of the photocathode to the high bandwidth diode array. The Digicon electrode potentials are adjusted to provide electron image magnification appropriate for the size of the target.

II. **Object Detection.** Upon detection of the surface flash, the gating grid is biased on to the full gain mode of operation. High bandwidth LIDAR data is collected by the diode array, amplified, digitized, and applied to a Maximum Likelihood detection processor. Upon object detection, the tube is gated totally off, and a timing signal is generated to allow the gating grid control necessary to turn the tube on with the next laser pulse at the gate which coincides with the object depth.

III. **False Alarm Mitigation/Classification.** In this phase the deflection coil is deactivated and the tube potentials are adjusted to image the photocathode at the appropriate magnification onto the CCD array at the center of the Digicon tube. At the appropriate instant the tube is gated on allowing a range gated image of the object to be collected by the CCD array. That image is then available for automated processing or human observation. With an inertially stabilized, gimballed scanning mirror, multiple images can be generated with multiple laser pulses to improve the Image SNR by integration or to assemble a mosaic view of larger objects which cannot be fully imaged with a single pulse. This could be performed digitally off-chip or by on-chip charge integration.

To perform the IFF function for large objects detected at large scan angles, it may be

necessary to generate multiple sequential gates of high resolution imagery because of the inability to capture the entire object extent within a single narrow gate. With the gated CCD camera used in Phase III this can be accomplished by directing multiple pulses toward the object, with the CCD gate-on timing adjusted to provide a sequence of gated images which encompass the entire object. To generate the three dimensional data base required for IFF, this procedure may require more laser pulses than a large array of high bandwidth detectors. The penalty associated with this less efficient use of laser power is in fact very small because it is incurred only during the small fraction of time when the system is being used in the IFF mode of operation, after detection of the large target has been established.

3.0 DETECTOR SUBSYSTEM DESIGN

In this section we summarize the status of the design of the dual-mode Digicon detector and its associated hardware. Key features of the dual-mode Digicon are the use of the GaAs photocathode for high quantum efficiency (Q.E.), the use of the APD array to obtain high gain and good signal levels for the time-resolved detection mode and the direct use of a CCD array in the tube to obtain high spatial resolution for the identification mode. ***When compared with range-gated cameras using conventional micro-channel plate (MCP) intensifiers, the dual-mode digicon benefits from a substantial improvement in detector noise factor. When combined with the higher Q.E. of the GaAs photocathode, these benefits generate nearly a 10 dB improvement in image SNR.*** These benefits are summarized in Table 3.1.

Table 3.1 Dual-Mode Digicon SNR Advantage Over Conventional MCP

	MCP	DMD	DMD SNR ADV.
NOISE FACTOR	3.0	1.0	4.8 dB
Q.E.	0.12	0.3-0.4	4.8 dB
TOTAL SNR ADVANTAGE FOR DMD OVER MCP			9.6 dB

3.1 Photocathode

The GaAs photocathode will be fabricated by the EO Sensors Division (EOS) of Intevac Corporation (formerly the EOS Division of Varian). The photo-response of the GaAs photocathode in the field assisted mode is dependent on the applied electric field, as illustrated in Figure 3.1. The quantum efficiency of the blue-enhanced GaAs photocathode versus wavelength is given in Figure 3.2. The figure gives the quantum efficiency for three applied electric field strengths, the maximum used in the experiments of about 50 kV/cm, the 1.5 kV/cm

which is used in the standard Digicon and 11.7 kV/cm which is approximately the field strength required to exceed a quantum efficiency of 30 percent at 532 nm. The last operating point was chosen as the goal for the program to develop the GaAs/APD Digicon as a performance upgrade detector and is a reasonable goal for the dual-mode detector.

The GaAs photocathode is activated with cesium and tends to be very sensitive to contamination and to have a risk of short lifetimes, especially at elevated temperatures, which can cause the cesium to migrate from the photocathode to other parts of the tube. The shelf life of the GaAs photocathode in a large-volume Digicon tube has been demonstrated by EOS on five tubes which were fabricated under the NRL laser radar detector technology program. The evaluation Digicons did not include a grid which could be used for demonstrating the field-enhanced performance of the photocathode. However, the quantum efficiency of the tested tubes was consistent with the plots for the "standard" Digicon given in Figure 3.2. The photo-response of the five tubes in microamperes per lumen versus months at room temperature is given in Figure 3.3. The two tubes which were fabricated first, 7B25 and 7B29, show relatively stable photo-response for periods between nine and ten months which is the total elapsed time since fabrication.

A second important issue is the thermal stability of the photocathode at elevated temperatures. It is often assumed that the mechanism for cathode degradation is a thermally activated process. We know that this is not strictly true; for instance, a tube response can be falling at room temperature and still recover at 100 C. However, the reaction kinetics of trapped gases or excess cesium inside a sealed tube is clearly temperature dependent. Although it may not be in the strict Arrhenius dependence of a negative exponential with a single activation energy, it is a rare occurrence when an increasing temperature does not accelerate the change in photo-response, whether the response is increasing or decreasing. To evaluate this phenomenon, EOS baked three of the large-volume tubes at 100 C and checked the photo-response between bakes. For comparison, two EOS standard ANVIS Generation III night vision tubes were put through the same process. Figure 3.4 gives the photo-responses versus bake time in hours at 100 C. Clearly the results show that the three large-volume tubes, 7A28, 7A33 and 7B28, showed

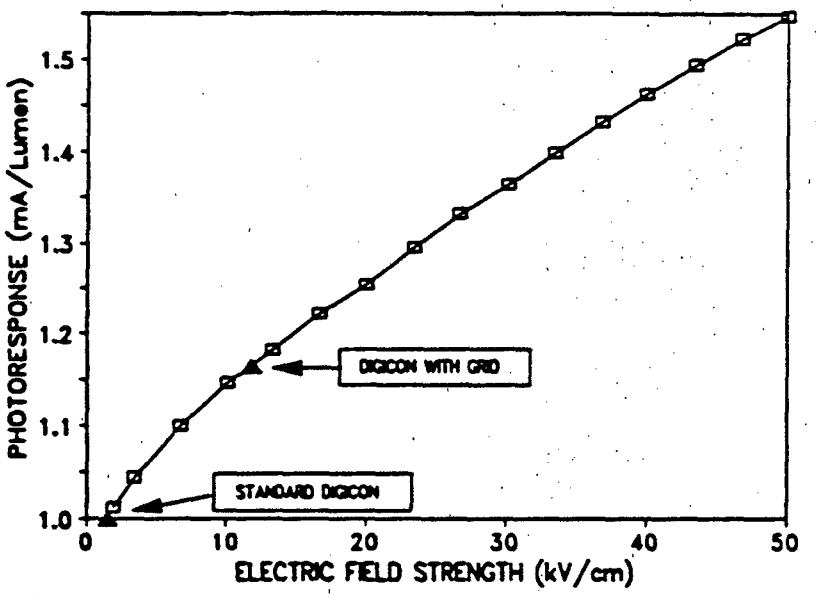

Figure 3.1 GaAs Photocathode Response versus Electric Field

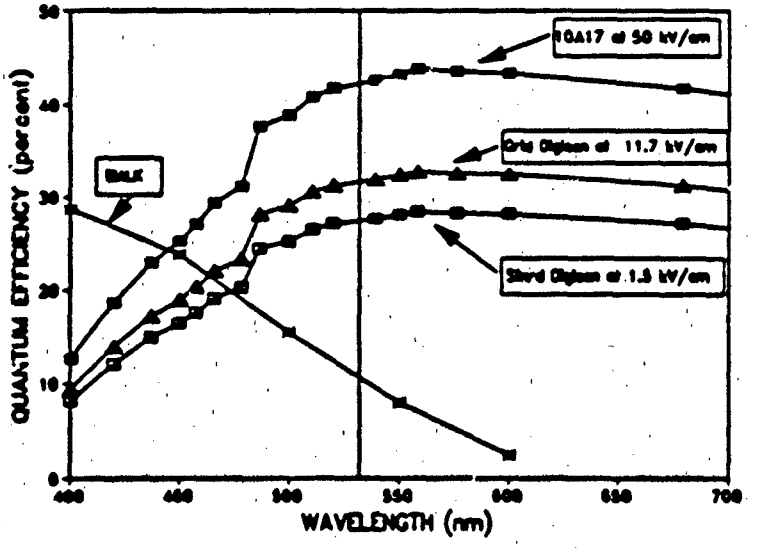

Figure 3.2 Quantum efficiency of GaAs Photocathode

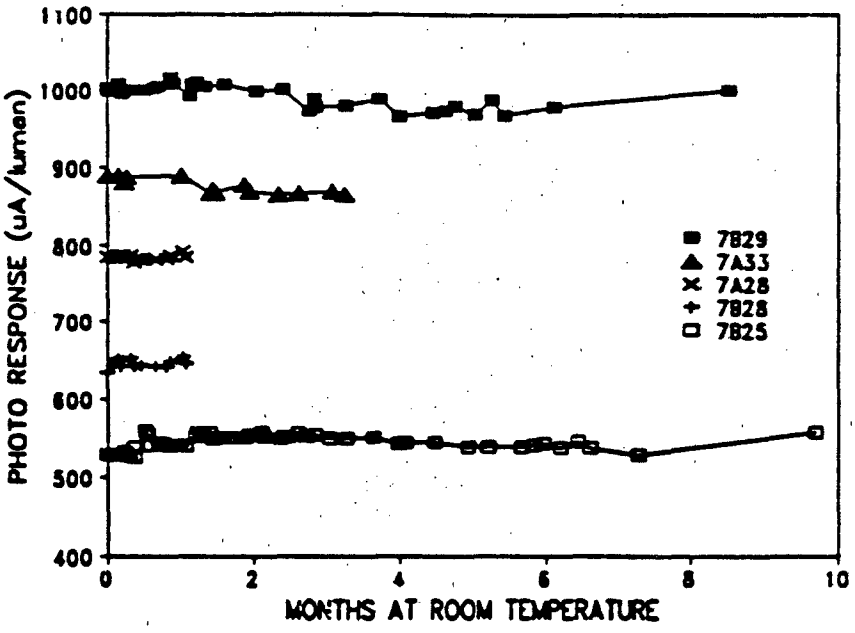

Figure 3.3 Photo-Response of GaAs Photocathode vs Months After Fabrication

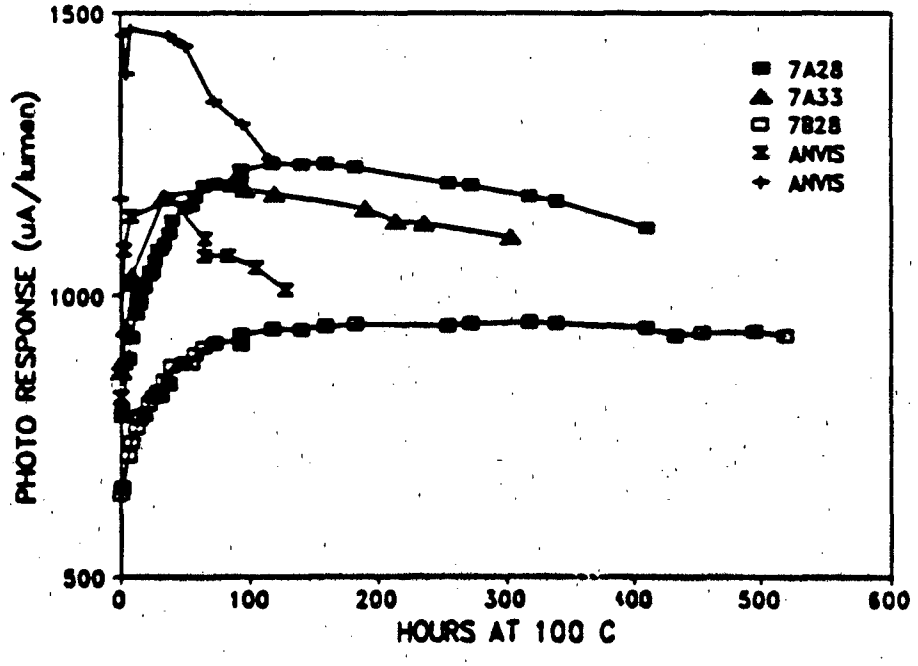

Figure 3.4 Thermal Stability of GaAs Photocathodes at 100 C

exceptional stability at elevated temperatures, exceeding the stability of the small-volume night vision tubes.

3.2 Photocathode Cooling

The dark-current for the high performance GaAs photocathodes at the full 50 kV/cm is illustrated in Figure 3.5. The current density in electrons per nanosecond per square cm is plotted versus inverse temperature in electron volts. The value of the temperature in degrees C is also indicated on the abscissa for a number of discrete values. The straight line fit of the data on a semi-log plot indicates the relation $I = A \exp[-E_a/kT]$, where A is a constant, E_a is an activation energy, k is the Boltzmann constant and T is the absolute temperature. The straight line in the figure extrapolates the dark-current to the higher temperatures which are of interest in an operational system.

We have used the values from Figure 3.5 for the photocathode dark-current in the SAIC computer model to evaluate the effect of the photocathode temperature on the signal-to-noise (SNR) performance of the overall receiver. The results are illustrated in Figure 3.6. The results in the figure show the beginning of a significant drop in SNR at a photocathode temperature between 40 and 50 C. In order to maintain a high SNR, we plan to actively cool the GaAs photocathode to about 40 C during operation. Based on the exceptional stability of the photocathodes in the Digicon tube at temperatures of 100 C for over 500 hours, as shown in Figure 3.4, one expects good storage lifetimes at temperatures up to 70 C or greater. The level of dark current from the high-performance GaAs photocathode requires that the photocathode be cooled to between 40 and 50 C, in order to maintain a high SNR performance in the receiver. We have developed and evaluated a concept for providing the necessary cooling for the photocathode of the Digicon. The conceptual design, which is illustrated in Figure 3.7, uses a copper strap and collar to connect thermally to the photocathode. The copper strap conducts the

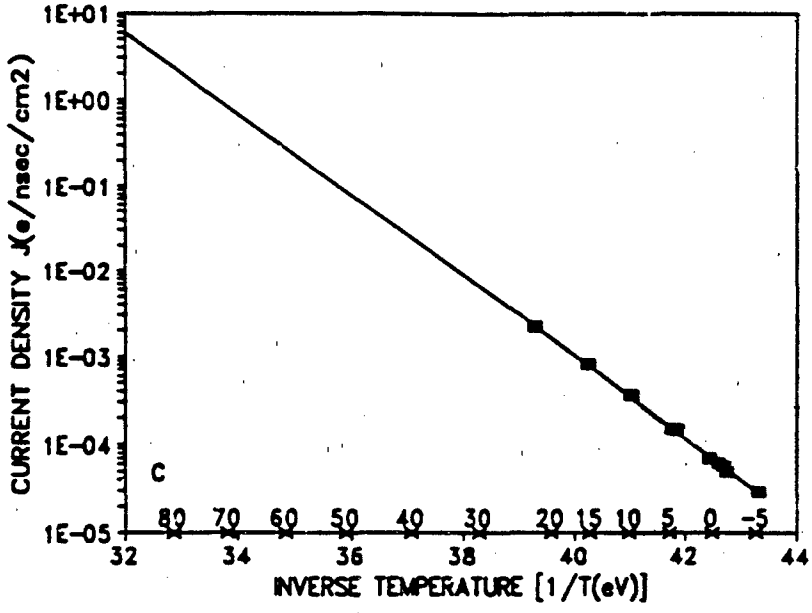

Figure 3.5 GaAs Photocathode Dark Current vs Temperature

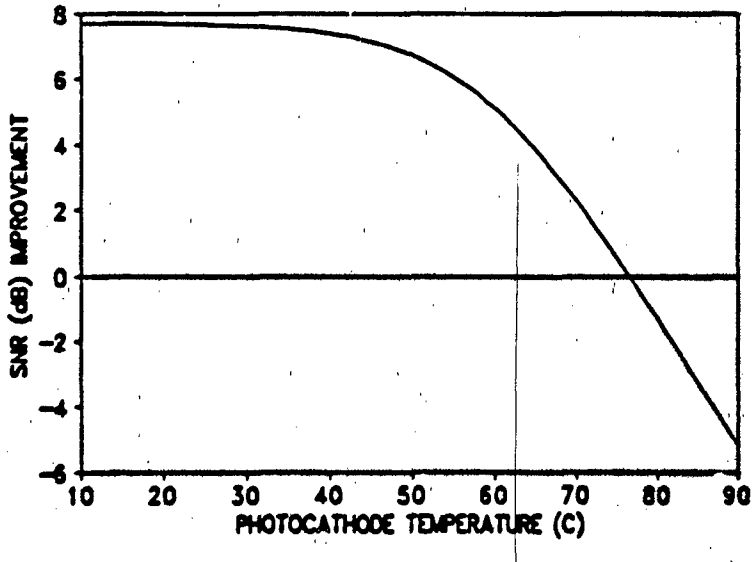

Figure 3.6 Detection SNR vs Temperature of GaAs Photocathode

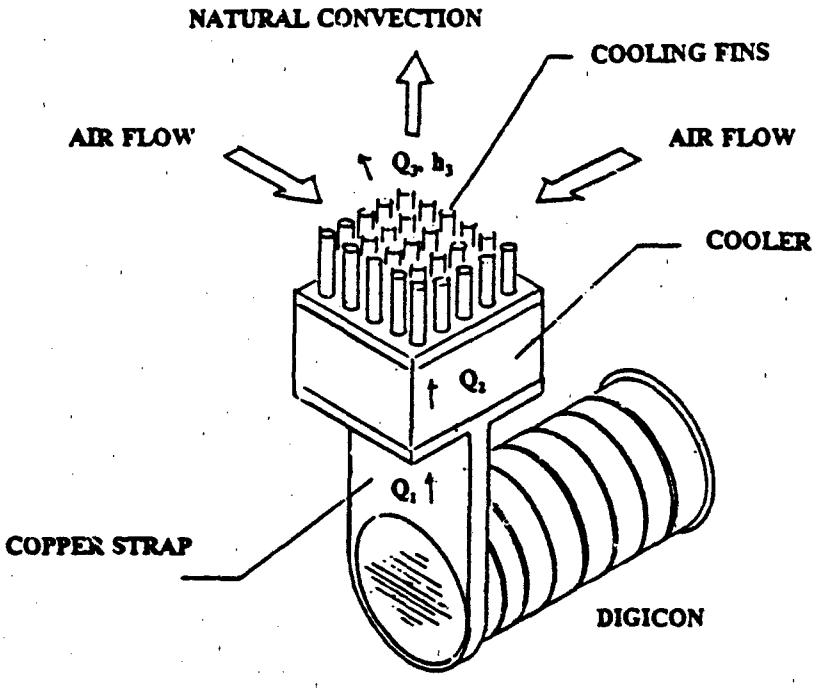

Figure 3.7 Cooling Design for Digicon Photocathode

heat to the cool side of a thermoelectric cooler. The heat exhaust side of the thermoelectric cooler is attached to a number of cooling fins which are located in the air ducts of the pod containing the sensor system.

We have performed an analysis of the thermal response of the system with and without the deflection coil activated. The results are summarized in Figure 3.8. To determine the power required to cool the photocathode to a specific temperature, begin with the required photocathode temperature on the left ordinate axis, then read the required cold-side temperature of the thermoelectric cooler on the abscissa. Using this value of the abscissa, the total parasitic heat load in watts can be determined from the ordinate axis on the right. For example, to cool the photocathode to a temperature of 22 C requires a cold-side temperature of about 20 C and approximately 5.6 watts of input power to the thermoelectric cooler. The two separate lines appearing in these plots correspond to the deflection coil being passive or active. The additional heat load generated by the deflection coil is negligible.

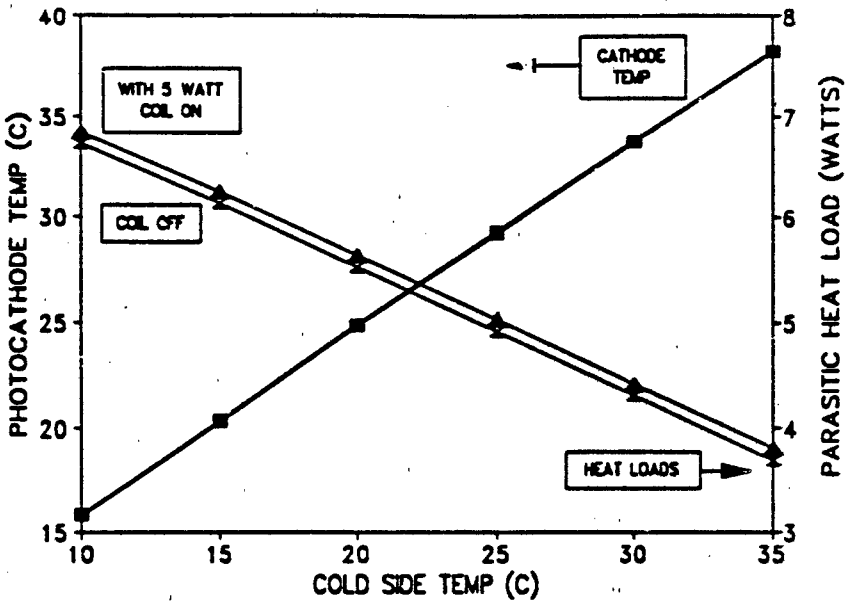

Figure 3.8 Parasitic Heat Load for Cooling GaAs Photocathodes

3.3 Gating Grid

EOS has previously operated gating grids in small-volume tubes used in night-vision devices. These grids have also been used to achieve high electric field strengths at the photocathode to obtain the high field-enhanced quantum efficiencies as given in Figure 3.2. The gating grids are etched from a thin, flat plate of a metal such as copper. This gives a high electron transmission efficiency with a relatively rigid mechanical structure due to the grid thickness in the direction of electron propagation. No problems are anticipated for incorporating a gating grid into the dual-mode Digicon. There is an unresolved issue that the uniform potential surface of the gating grid may distort the electric focus fields near the photocathode and disturb the quality of the electron image at the diode array, especially in the identification mode where the high-resolution CCD is the electron detector. This issue will be addressed in the present NRL

program using one of the test Digicon tubes with a gating grid and a phosphor screen for direct viewing of the electron image.

3.4 Electron Optics

In an internal research and development program, SAIC has developed and demonstrated an electrostatic focussed Digicon with a high quality electron image at the anode. The concept was developed for the same Digicon tube configuration as used for the Hubble space telescope and the NRL 8x8 Digicon for laser radar. The tube configuration uses a 30 mm photocathode and a 150 mm long tube body. The maximum diameter for a GaAs photocathode which can presently be fabricated by EOS is 25 mm. The EOS processing stations can accommodate a tube about 100 mm in length. Furthermore, it is desirable to reduce the overall size of the Digicon tube to save space in the sensor receiver.

For the above reasons, we have evaluated the imaging properties of a smaller Digicon tube which also has a smaller length to diameter aspect ratio. Using the EGUN code for electron trajectories in a mini Digicon, it was found that the electron image has a significant amount of distortion at anode radial distances of 6 mm. The local value of the tube magnification versus radial distance at the cathode is illustrated in Figure 3.9. The large variation in image magnification versus electron ray height results in severe pin-cushion distortion, which is illustrated in Figure 3.10.

In order to maintain the small size of the Digicon, but improve the quality of the electron image over a larger portion of the 25 mm photocathode, we have investigated a tube concept which uses nested cones, as shown in Figure 3.11 instead of simple flat annular plates as the tube baffles. Preliminary analyses of the electron image for this configuration is illustrated in Figure 3.12, which shows the image magnification versus cathode radial distance. The variation from the nominal value of M = 1.5 goes from a minimum of 1.44 to about 1.56 at a radial distance of 6.4 mm. This amounts to a variation of plus or minus about 4 percent in the magnification out to a radial distance of 6.6 mm at the photocathode, which for a tube magnification of 1.5

corresponds to a distance of 9.9 mm at the anode. For comparison, note that the corner of a 256x256 CCD with 20 micron pixels is located at a radial distance of 3.62 mm. The distortion map shown in Figure 3.13 continues to show some pin-cushion distortion, but it is significantly reduced. Additional trades between Digicon tube dimensions, tube aspect ratio and electrostatic focussing configurations are expected to further reduce the small amount of residual distortion. A small amount of distortion is easily removed by the signal processing computer.

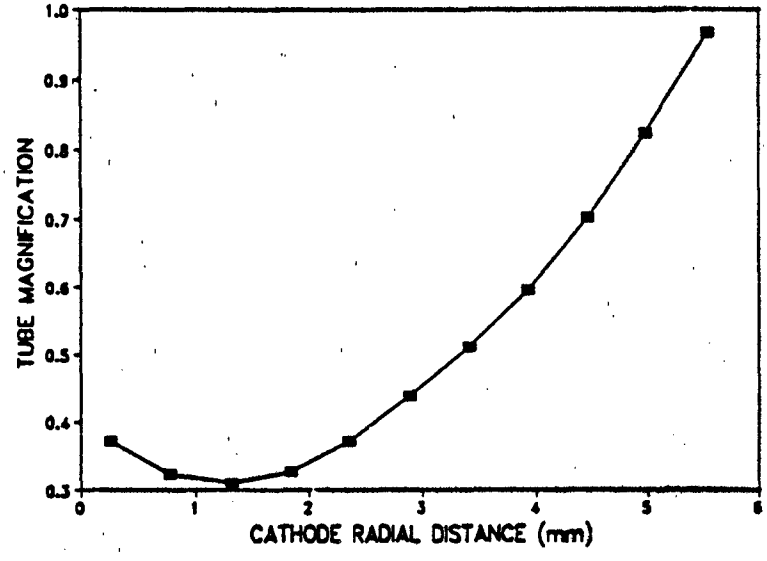

Figure 3.9 Electron Image Magnification vs Ray Height in Mini-Digicon

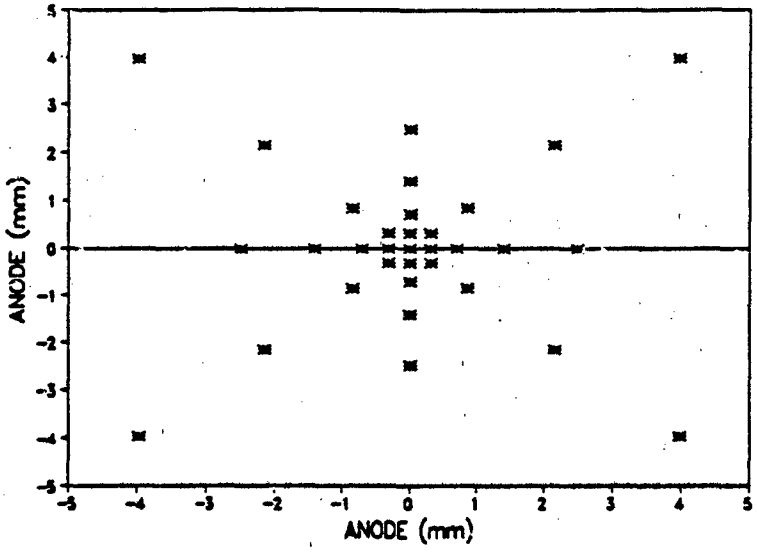

Figure 3.10 Electron Image Distortion in Mini-Digicon

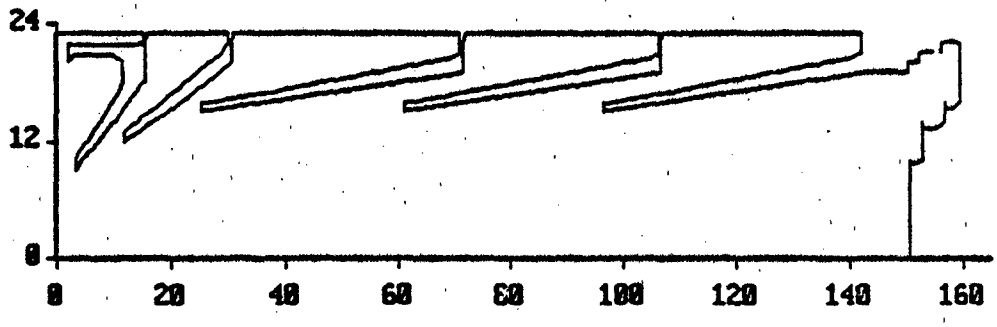

Figure 3.11 Electrostatic Focussing via Nested Cones

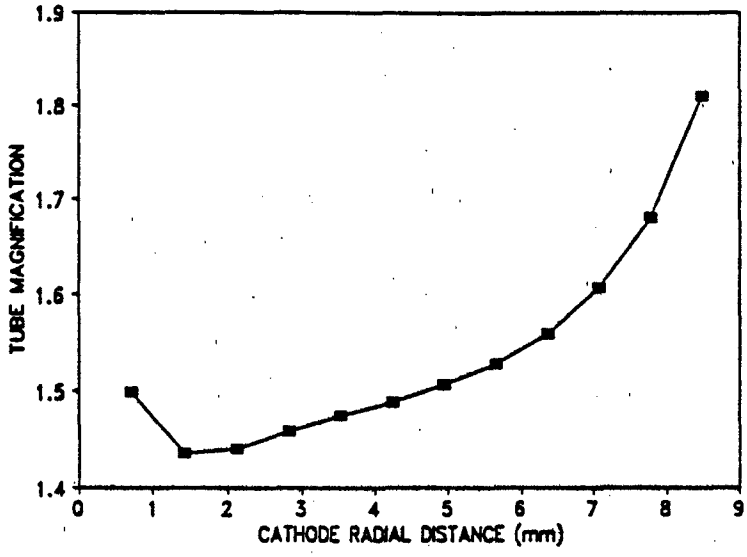

Figure 3.12 Image Magnification vs Ray Height with Nested Cones

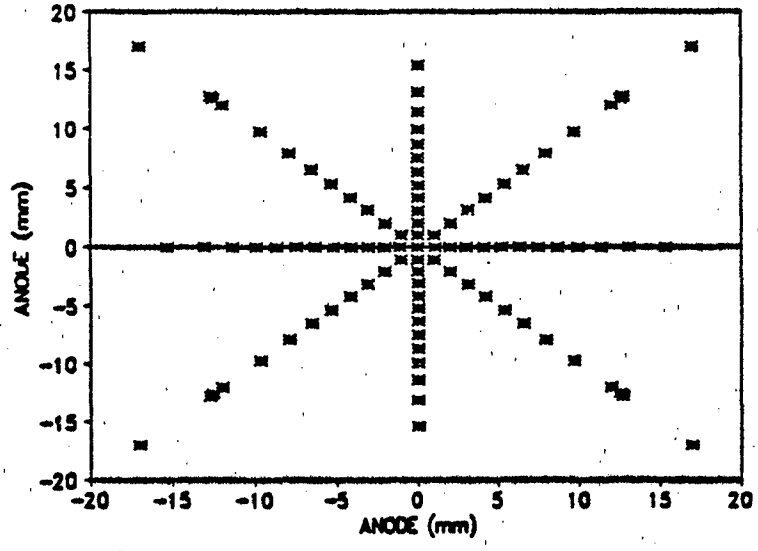

Figure 3.13 Electron Image Distortion with Nested Cones

3.5 Dual-Mode Digicon Header

To provide flexibility for use of the header to support future requirements, we have designed a header with 72 signal traces. The header design, as shown in Figure 3.14, will support the single element APD Digicon for the performance upgrade, the dual mode Digicon with APD quad and CCD arrays or the Digicon with 8 x 8 parallel channels. The header is also designed to interface with a standard, commercially available zero-insertion-force (ZIF) socket. This will facilitate integrating the Digicon tube into the receiver subsystem.

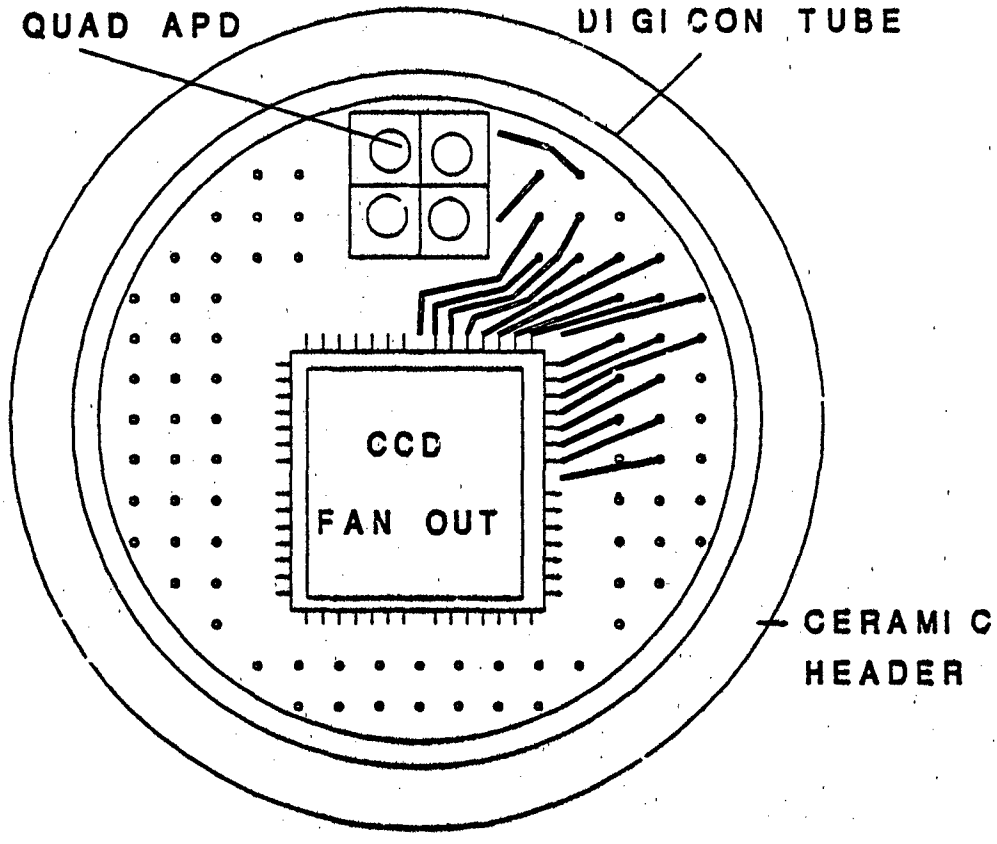

Figure 3.14 Tube Header for Dual-Mode Digicon

3.6 Avalanche Photodiode (APD)

As a part of their standard product line of silicon avalanche photodiodes (APD), E.G.&G. manufactures a quad-cell APD, part number C30927E. The standard quad-cell is supplied in a TO type can as are most of their other APD's. E.G.&G. is presently under contract to SAIC to characterize electrically the performance of their APD before and after thermal cycling to simulate a complete tube fabrication thermal bake. E.G.&G. is also evaluating two high-temperature eutechtics to be used in die attachment procedures for the APD. Samples of the APD will also be used to test the effects of using an electron scrub procedure in the final Digicon tube fabrication. Successful completion of this effort will allow the purchase of these diodes in chip form for use in SAIC Digicon tubes. The diodes are specified with a 3 nsec risetime yielding more than adequate bandwidth for the present application. The surface area of each cell of the quad is approximately 1.3 mm^2. The dark current is specified at 25 nA and the spectral noise density is 0.5 $pA/(Hz)^{1/2}$. Previous calculations for these APD parameters, when used as the electron detector in a Digicon tube with EBS gain of about 5,000, indicate that single photon counting can be achieved with reasonable margin.

For the performance upgrade using a single pixel APD Digicon, we have identified two candidate APD's based on standard devices: E.G.&G. part number 30916 and Hamamatsu part number S2384. The Hamamatsu device uses p type material with n type depositions. Hamamatsu does not expect any degradation due to the thermal bake at 360 C for 24 hours which is required for tube fabrication. Ten APD devices have been purchased for evaluation. Hamamatsu is also providing ten modified devices to reduce the boundary layer which results from the doping to provide the bias and the passivation of the surface. The goal of the reduced boundary layer is a thickness of 0.5 micron. Both devices will be tested. The Hamamatsu device is ready for die attaching to the header and wire bonding for the bias and signal traces.

In the APD detector, the EBS gain of about 5,000 is coupled with the avalanche gain. Even though the avalanche gain has a higher noise factor, the composite noise factor for the product gain, EBS times avalanche, is expected to be low. In the same manner that a high-gain

first section is used in a multiple stage photomultiplier tube to reduce the effective noise factor, the high gain EBS stage of the APD Digicon can reduce the effect of the APD noise. In the Digicon with an ordinary silicon diode for the electron detector, we have experimentally demonstrated a near-linear response over about five orders of magnitude of input signal. We have also experimentally demonstrated that the Digicon will recover from a large amplitude, short duration input pulse in less than 20 nsec. In short, the pulse recovery characteristics and dynamic range of the Digicon detector with electron input to the silicon diode is virtually identical with the performance of the silicon diode when it is directly excited by an optical input which [illegible]

electrons or ultraviolet light is required to remove excess silicon from the substrate so that the short range radiation results in charge deposition in the CCD wells.

One of the technical concerns is the life of the CCD under bombardment by 15 kV electrons. Some insight to this issue is gained by comparing the range of electrons in silicon, which is illustrated in Figure 3.15, with the thickness of silicon in a thinned CCD, which is illustrated in Figure 3.16. The electron energy deposition data show that the range of a 15 kV

...microns. The thinned CCD has a p type epitaxial layer

...ons between the incident photoelectrons and the n type

...ion from the photoelectrons in the region of the gate

...d Reinheimer of Tektronix Laboratories have addressed

...D's as electron detectors at energies between 1 and 10

...unction as both and efficient and robust electron imager."

...eedings Vol. 1447, February 1991.

...ability to design and thin CCD's fabricated to our

... formerly Ford Aeronutronics. Array sizes can range from

...ional sources of backside thinned CCD chips which are

... Digicon tube processing have been identified. Tektronix

...arrays, while Phillips manufactures a 604 x 288 array.

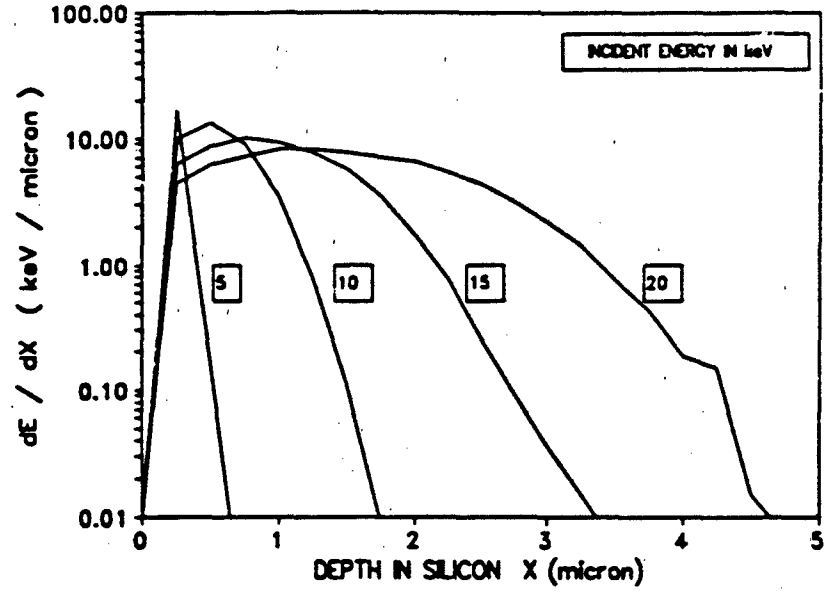

Figure 3.15 Electron Energy Deposition in Silicon

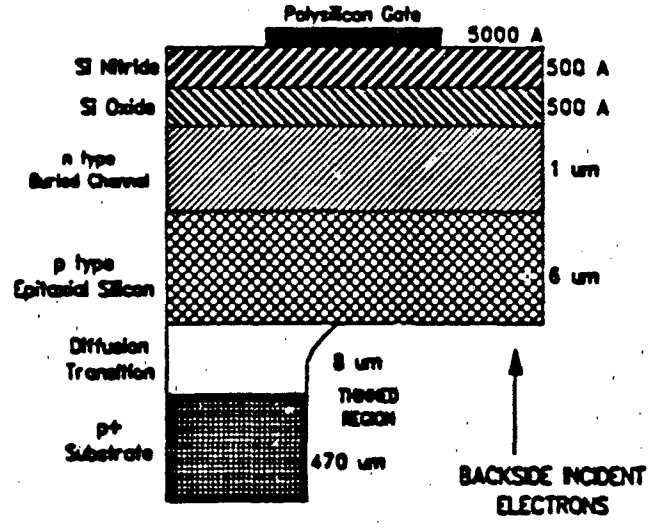

Figure 3.16 Thinned CCD for Backside Illumination

4.0 DETECTOR ELECTRONICS SUBSYSTEM

The electronics subsystem provides processing of the received signals and control of the Dual-Mode Digicon detector. The electronics subsystem is packaged in the immediate vicinity of the detector to insure the highest signal integrity and to provide the high-speed and short delay times needed for control. Location of both the signal processing and control electronics with the detector provides the required integrated functioning of the detector subsystem. The block diagram of the electronics subsystem is shown in Figure 4.1.

4.1 Signal Processing Electronics

Signal processing electronics provide the following functions to support both the high bandwidth and the high resolution modes of operation:

1) High-speed, low-noise amplifiers for each APD channel. These amplifiers provide dynamic range compression such as the logarithm function it insure the dynamic range of the digitizer is not exceeded. The inverse of the compression function is applied in the digital processing so correct radiometric data is available.

2) The high-speed digitizer provides continuous waveform digitization of the return signal from the APDs from the surface to the maximum detection depth. Available flash ADC's (analog-to-digital converters) can operate at up to a 30 MHz rate and provide 8 to 10 bits of accuracy. A separate ADC is used for each detector channel.

3) The surface flash detection circuit provides the trigger needed to switch to the enhanced gain of the photocathode. The timing of the received surface flash is recorded for accurate calibration of the depth of objects detected on the high bandwidth channels. The surface flash detection threshold is set by the analog control unit.

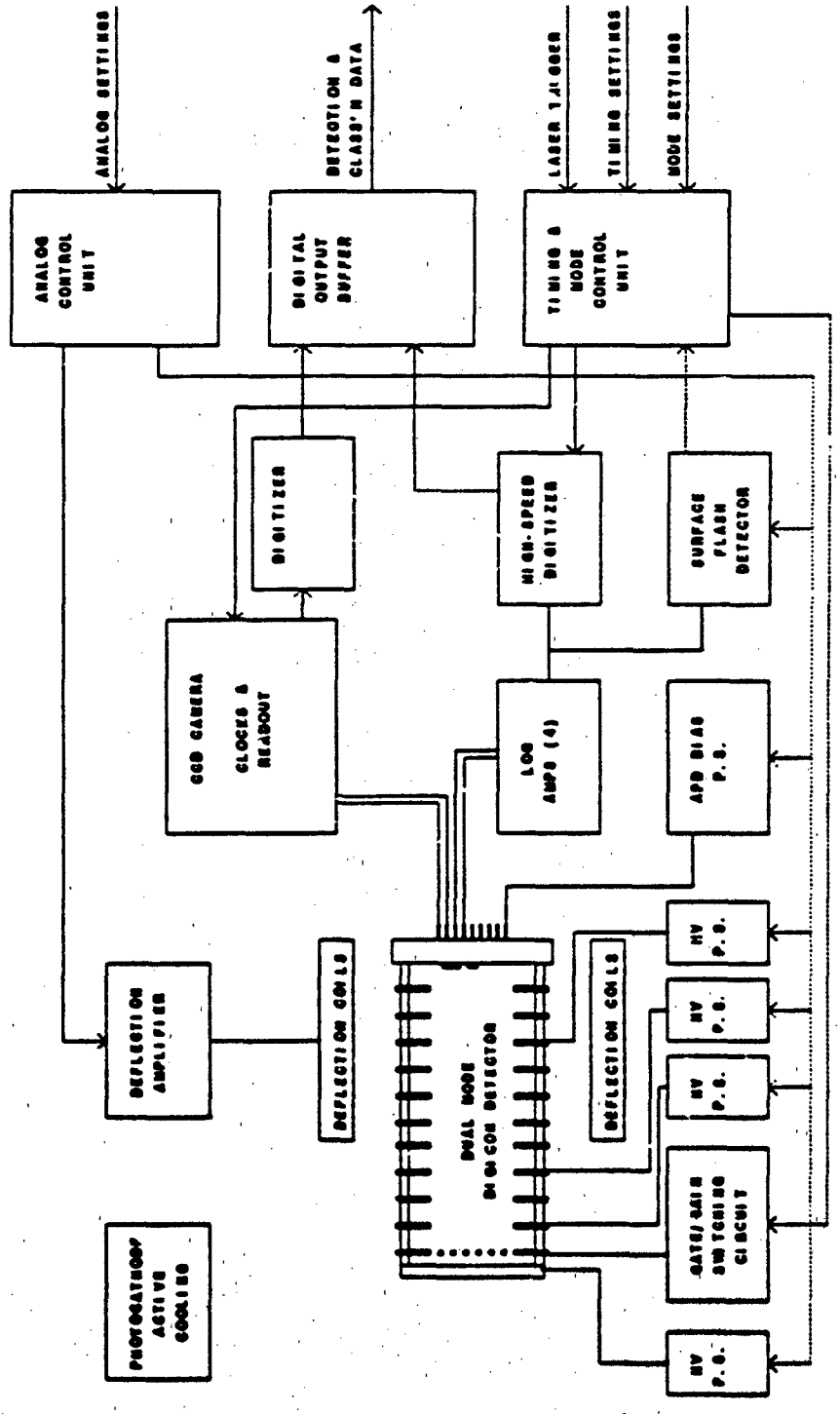

Figure 4.1 Electronic Subsystem for Control of Dual-Mode Digicon and Signal Processing

4) A conventional CCD camera electronics package provides the signal readout in the high resolution mode. Phase clocks are provided to the CCD parallel and serialregisters t allow the analog pixel samples to be read out with the various binning factors.

5) A larger dynamic range of 12 to 14 bits is used for the digitizer in the high resolution mode to account for the low readout noise and the large samples encountered when binning is used. The larger dynamic range is offset by the reduced 2 to 5 MHz conversion rate requirement.

6) A digital output buffer is provided in both modes of operation. The digital output buffer for the high bandwidth mode is up to 256 samples deep for each channel. This is sufficient to store all the samples received from a single shot of the illumination laser. Data is written at the 30 MHz ADC rate and then read out at a lower rate for detection processing. In the high resolution mode, data is written at the slower rate but 64 kilo-words of memory is required. The data buffer is the interface to the host computer system.

4.2 Detector Control Electronics

The detector control electronics provide the proper configuration of the detector for each shot of the laser. Commands from the host computer system and laser trigger are received by the electronics subsystem and used to setup the various control components described in the following sections:

1) The timing control unit performs the high speed sequencing needed for sensor operation. This unit provides delays from one action to the next with nanosecond accuracy. The various delay settings are received from the host computer before the illumination laser is fired. The beginning of the photocathode gate and high-speed digitizer periods are controlled by delays from the laser trigger pulse. The change to

enhanced photocathode is controlled by a delay from the surface flash detector output. A signal is also provided to the CCD camera electronics to initiate the data readout.

2) The tube gate and gain switching circuit controls the voltage on the grid immediately behind the photocathode. When the tube is off the grid is held at a potential below the photocathode potential. The gating grid potential is raised above the photocathode potential to turn the tube on. Increasing the grid potential further creates a high gradient at the photocathode thereby increasing the quantum efficiency. This circuit is located as close as possible to the Digicon tube because of the short switching times and the requirement to switch a voltage of the order of 200 V at a level of about 15 kV. The switching circuit receives control signals from the timing control unit.

3) The analog control unit receives digital commands from the host computer and provides analog control signals to several power supplies and amplifiers in the detector subsystem. The timing of these settings is not critical because they are changed between shots of the illumination laser which is typically 5 to 10 msec.

4) The deflection amplifier controls the current in the deflection coils based on the analog signal from the analog control unit. The proper current settings to center the electron image on each of the anode detectors are determined during sensor calibration.

5) Three or four high voltage power supplies are provided to control the imaging and magnification fields in the Digicon tube. High accuracy power supplies are required to provide both the large voltage changes to control the magnification and the small voltage changes to adjust the focus. The control signals are received from the analog control unit.

6) The APD bias power supply is also controlled by the analog control unit. In addition to the bias voltage determined during sensor calibration, a closed loop monitoring system is used. The APD current is monitored periodically during the period when the tube is gated off (dark current) and the bias adjusted accordingly.

4.3 Electronic Subsystem Functions During Operation Cycle

The electronic subsystem performs a number of functions for each cycle of the illumination laser. These functions are sequentially listed below:

1) The host computer calculates or looks up the mode, timing, and analog settings that will be used on the next laser shot. The mode and analog settings are used immediately to set the proper image deflection, magnification and focus. The timing delays are calculated from the altitude and the angles of the scanning gimbals. The timing delay settings are used to preset counters in the high-speed timing control unit that are started by the laser trigger or the surface flash detector.

2) The signal that the laser has fired is received from a detector that samples that actual outgoing laser illumination pulse. The timing control unit sends a signal to the gate switching circuit after the proper delay.

3a) In the high-bandwidth mode the tube grid is turned on before the surface flash is received. The high speed digitizer is also started. The signal from the surface flash detector is delayed and used to shift the grid into the enhanced gain mode. The tube remains on until all the samples have been collected by the high-speed digitizer.

3b) In the high resolution mode the tube in gated on for a short period (10 to 50 nsec.) that corresponds the depth being searched. After the tube is turned off the CCD camera electronic package begins to read out the data into the output buffer.

4) Signal processing is complete when the high-speed memory is filled or all the image is read out from the CCD.

5) The data in the digital output buffer is transmitted to the host computer for waveform or image analysis.

5.0 RECEIVER TELESCOPE

In the conceptual design of the telescope for the sensor receiver, two approaches have been considered. In the first approach, the refractive afocal telescope of the present system is retained, with relatively minor modifications to the final focussing lens subsystem. In the second approach, a telescope with some reflective components is used to form directly an image plane in an attempt to reduce the total volume required for the optical subsystem. The features and status of these two approaches are discussed in the following.

5.1 Afocal Refractive Telescope

One of the advantages of the afocal telescope is the nominally collimated region following the telescope where a filter with a smaller aperture, corresponding to the magnification of the telescope, can be placed. However, it should be noted that the angular spectrum which must be handled by the filter has been increased by the same factor that the aperture diameter has been reduced. Thus the filter diameter is reduced, but the angular acceptance must be increased.

At the beginning of the conceptual design effort, it was desired to maintain the option to achieve the dual-mode receiver capability by using two separate detectors, one for the detection mode and one for the identification mode. In order to accommodate a detector switching component such as a flip mirror, we replaced the present 50 mm focussing lens with an 80 mm Mamiya 645 lens. As it turns out, progress on the reduction of risk of the dual-mode Digicon, along with the reduced volume requirements for a single detector, makes this single detector the preferred approach.

In order to evaluate the imaging capabilities of the existing afocal telescope across the field of view of the receiver, we have used a parabolic reflector as a perfect imager to focus the output of the afocal. For the evaluation of the afocal, the parabolic mirror is perfectly aligned with each off-axis ray bundle to eliminate aliment effects in the final focussing optic.The optical schematic is illustrated in Figure 5.1. The focal spot diagrams are given in Figure 5.2. From

the upper left, clockwise around the figure, the spot diagrams are for 1) on-axis, 2) 3.5 mrad off-axis, 3) 28.3 mrad off-axis and 4) 7.1 mrad off-axis. For reference, the spot-diagram angles of 3.5, 7.1 and 28.3 mrad correspond to the corners of squares with dimensions of 5, 10 and 40 m, respectively, viewed from a range of 1,000 m. Examination of the data in the figure shows that the dimensions of the focal plane spot for the largest 28.3 mrad angle is less than about plus/minus 0.04 mm. At 7.1 mrad, the spot size is less than plus/minus 0.01 mm. For comparison, the data in Table 2.2 for the identification mode give focal-plane pixel sizes of 0.5 mm for the large targets, 0.06 for the small targets and 0.016 for the very small targets. Noting that the half angle to the target plane for the very small targets is somewhat less that 28.3 mrad, the above results show that the present afocal telescope with an 80 mm lens more than meets the imaging requirements for the sensor under all currently specified conditions.

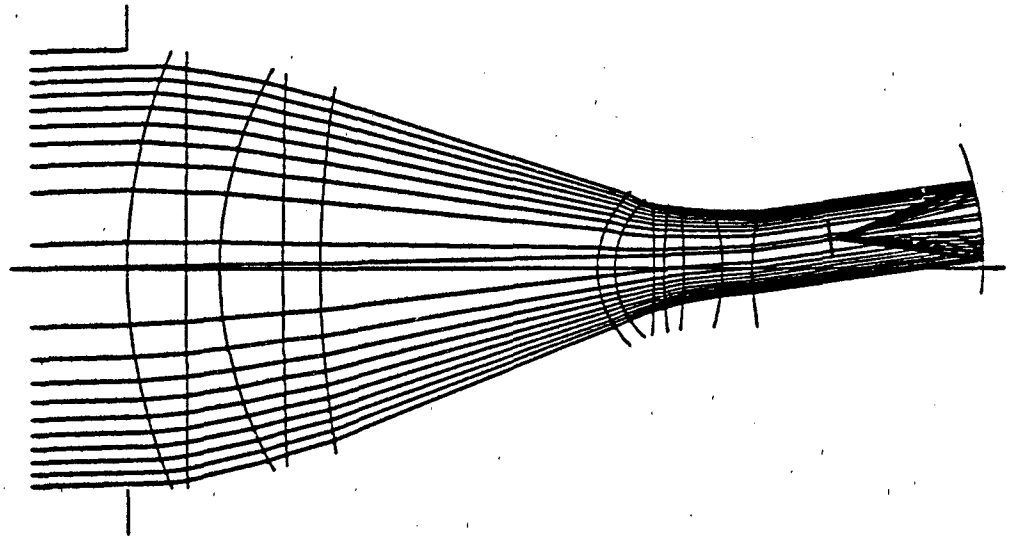

PARAMETER	VALUE
FOCAL LENGTH	0.40 m
APERTURE	230 mm
F-NUMBER	1.74

Figure 5.1 Optical Schematic of Afocal Telescope with 80 mm Lens

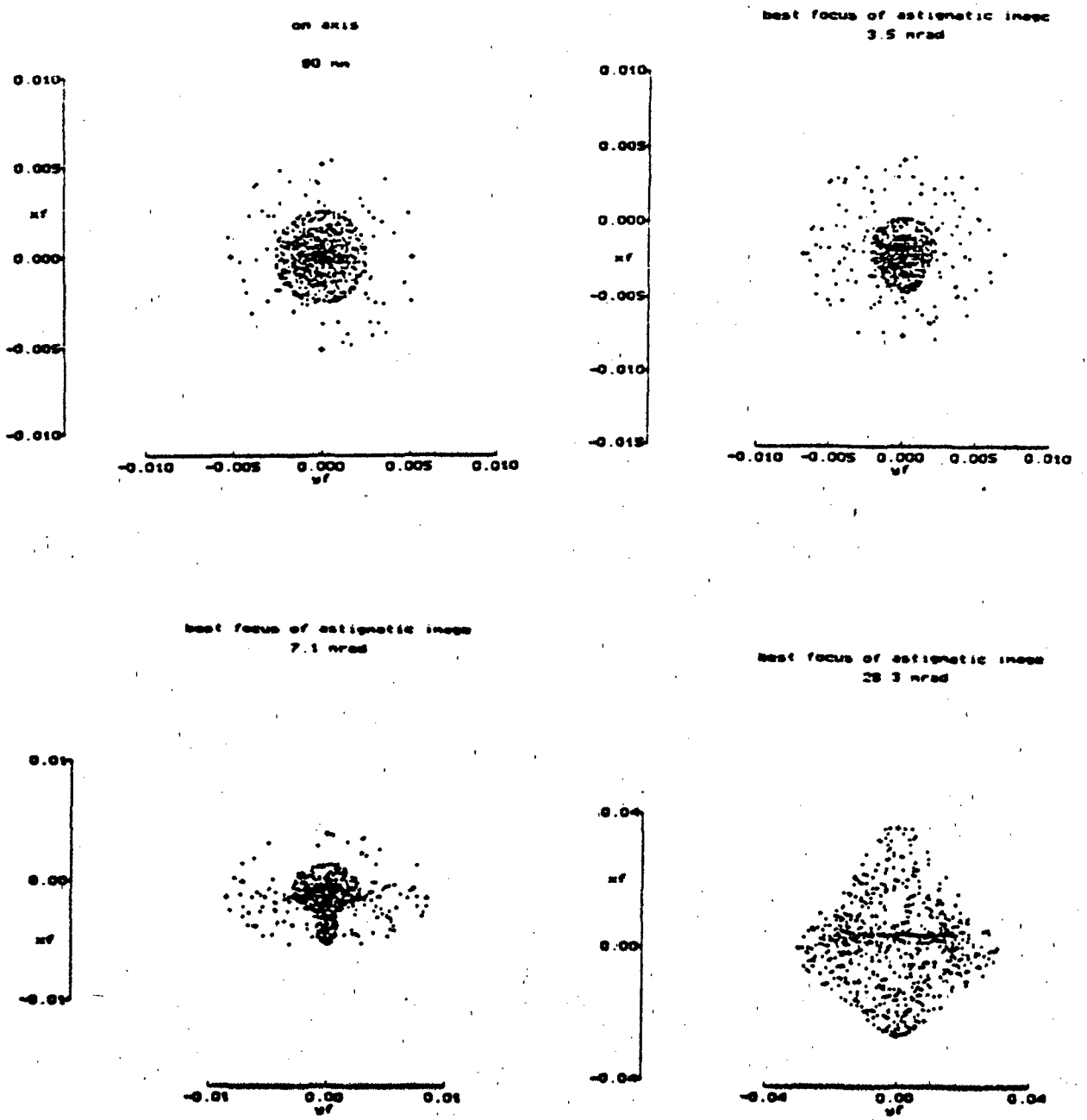

Figure 5.2 Afocal Telescope Spot Diagrams with 80 mm Mamiya "645" Lens

5.2 Gabor-Cassegrain Telescope

A critical parameter for integrating a dual-mode receiver or a time-resolved imaging array such as the 8x8 or 16x16 into the present pod is the volume required for the additional electronics. In order to save as much space as possible in the telescope, we have selected the Cassegrain hybrid developed by Gabor. The concept of the Gabor-Cassegrain hybrid telescope is illustrated in Figure 5.3. The telescope has the appearance of a folded Cassegrain, but with a figured refractive component as the first element. In our design, the focal plane is just to the right of the hole in the large reflector, which allows space for mounting the dual-mode Digicon. Based on the assessment of reduced risk for the dual-mode Digicon, an earlier version which could support two separate detectors was abandoned to save space.

Spot diagrams for the Gabor-Cassegrain telescope are given in Figure 5.4 with the same layout as Figure 5.2. Examination of the data in the figure shows that the image quality of the present hybrid design is not as good as the afocal telescope. However, even at the largest angle, which corresponds to the corner of a 40 m square at a range of 1,000 m, the spot dimensions are less than plus/minus 0.2 mm in both dimensions and the bulk of the spot energy is in an area with a radius less than 0.1 mm. Thus the hybrid will easily support detection and identification of the large targets and detection of the small targets over the entire field of view; see Table 2.2 for the pixel size requirements for the Gabor-Cassegrain telescope. Adequate resolution of 0.06 mm for identification of the small targets at the largest angle is marginal. However, at the corner of a 10 m spot with a 7.1 mrad angle, the radius of the spot containing the bulk of the rays is less than 0.05 mm which is adequate for identification of the small targets and detection of the very small targets. Identification of the very small targets with 0.017 mm pixels can be accomplished at the corner of a 5 m spot, corresponding to an angle of 3.5 mrad.

Based on the foregoing results, the Gabor-Cassegrain telescope is judged to meet the imaging requirements of the sensor system. As discussed in the following section, packaging considerations for the hybrid provide a strong motivation for its selection.

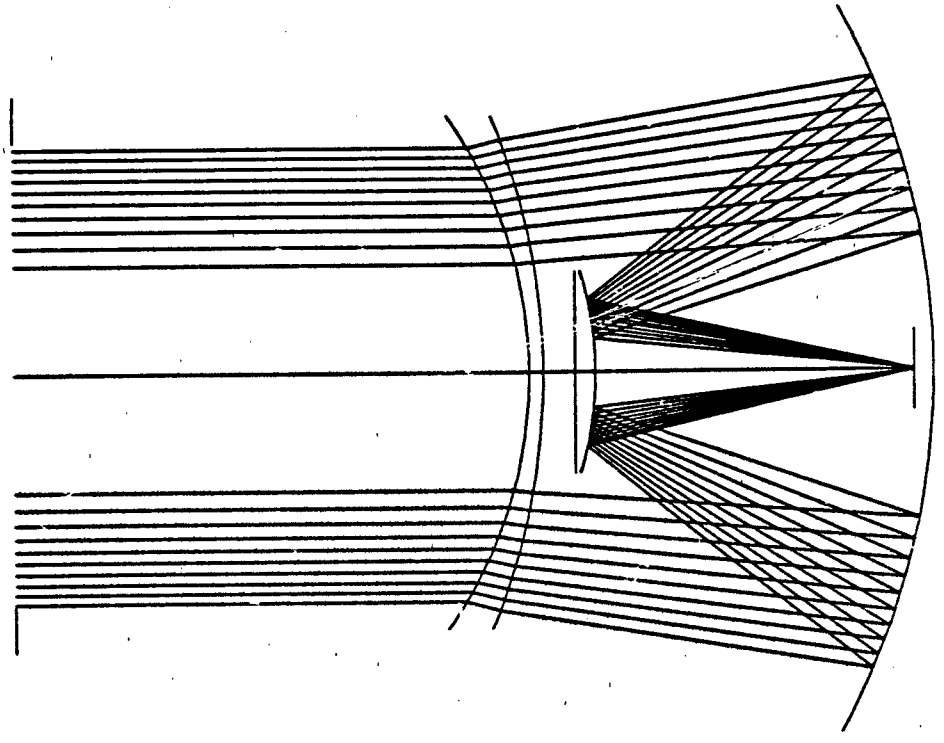

PARAMETER	VALUE
FOCAL LENGTH (mm)	445
APERTURE (mm)	219
F-NUMBER	2.0
TRANSMISSION EFFICIENCY (%)	82.6
PRIMARY MIRROR DIAMETER (mm)	304.8
SECONDARY MIRROR DIAMETER (mm)	91.4

Figure 5.3 Gabor-Cassegrain Telescope Configuration

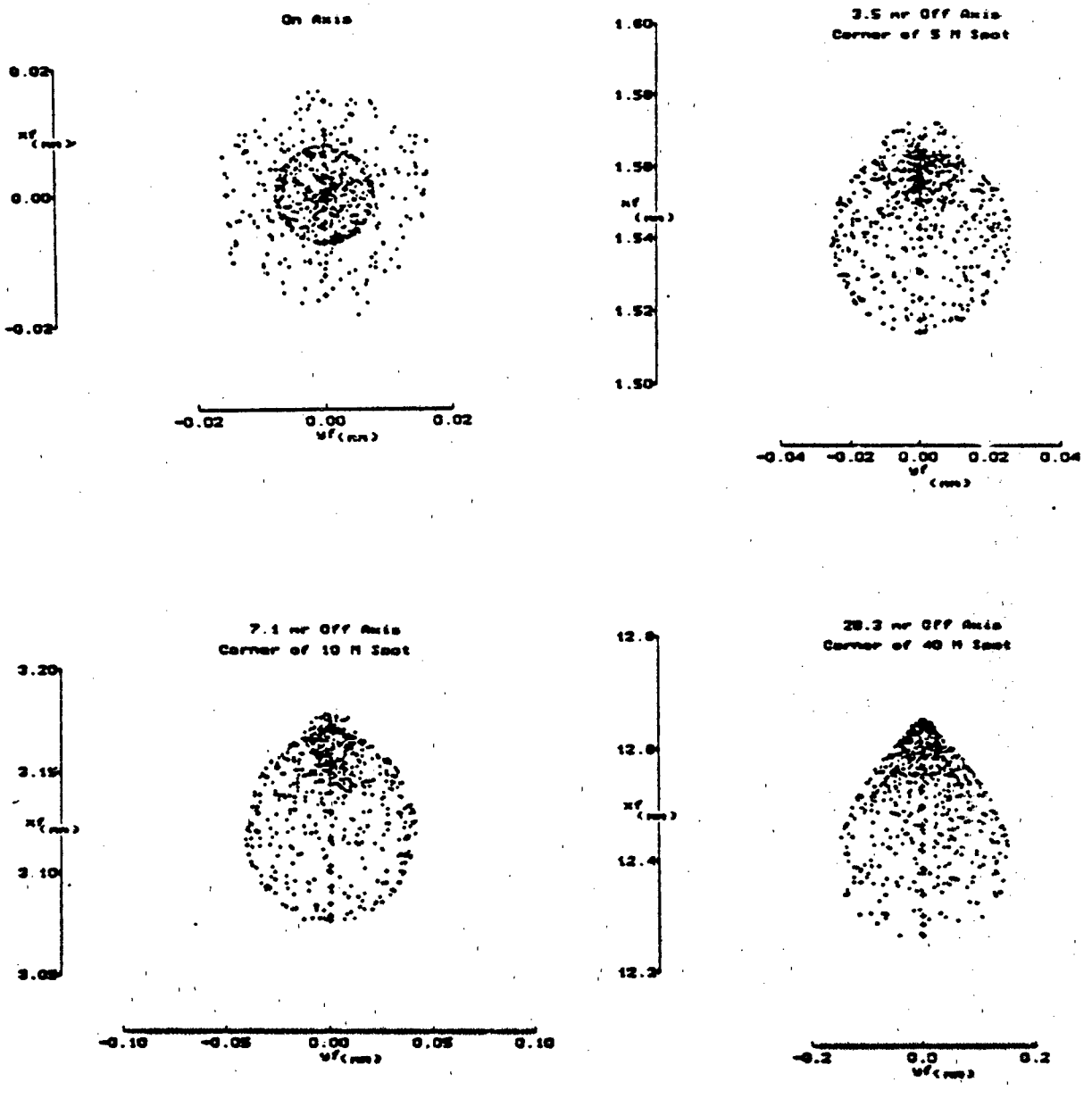

Figure 5.4 Spot Diagrams for Gabor-Cassegrain Telescope

6.0 RECEIVER PACKAGING

One of the principal objectives of the present conceptual design is to assess the ability to package the dual-mode Digicon receiver into an existing pod. The precise space required for the Digicon tube, power supplies, control circuits, and signal processing components is not presently known. However, it is clear that the space for the full dual-mode Digicon detector subsystem with four time-resolved channels and a range-gated CCD will exceed that required for the present subsystem which uses two photomultiplier tubes with two time-resolved channels. Assuming that the dynamic range of the Digicon will be sufficient that a single detector can be used, some space will be saved by replacing the two photomultiplier tubes and the beam splitting prism, which are used in the present system. Although this space is significant, it is expected that additional space must be made available for the dual-mode Digicon.

The present refractive, afocal telescope occupies a large portion of the volume of the receiver housing. To regain some of this volume for the required electronics, we attempted to use the Gabor-Cassegrain telescope with an approximately equal aperture in the existing receiver housing. The results are shown in Figure 6.1 a). In the figure the telescope is placed as far forward as possible without interfering with the scanning mirror in the forward scanner module. Clearly the primary reflector of the hybrid telescope interferes with the existing housing. However, with a relatively minor modification of the existing housing, the Gabor-Cassegrain telescope fits snugly within the module as illustrated in Figure 6.1 b). As the illustration shows, the modification of the housing consists of a slight steepening and rearward displacement of the tapered portion of the transition between the large diameter of the scanner module and the small diameter of the laser module. The modification does not affect the modules, but does require a minor modification of the sliding window cover for the scanner module.

The high geometric efficiency of 82.6 percent for the Gabor-Cassegrain telescope gives an improvement in light gathering over the present refractive telescope and lens due to the relatively large accumulation of low losses in a large number of optical components. More importantly, the volume saved by using the Gabor-Cassegrain is approximately 2,800 cm^3, or

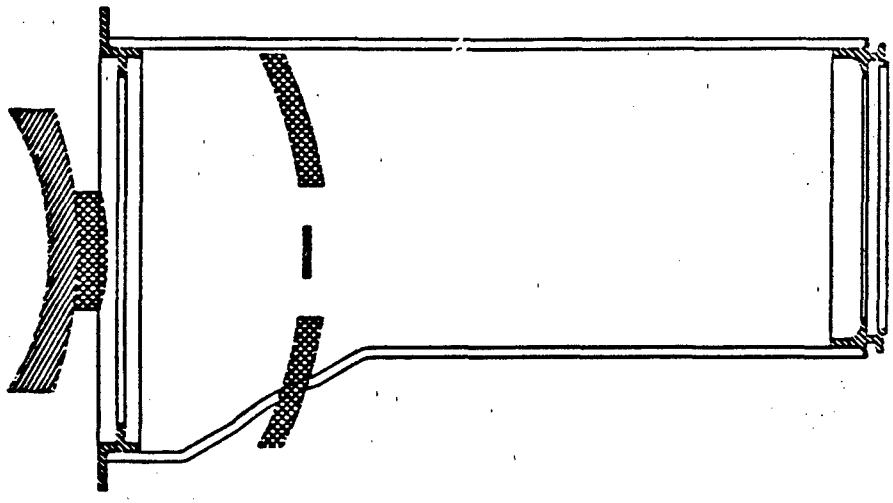

a) With Present Receiver Housing

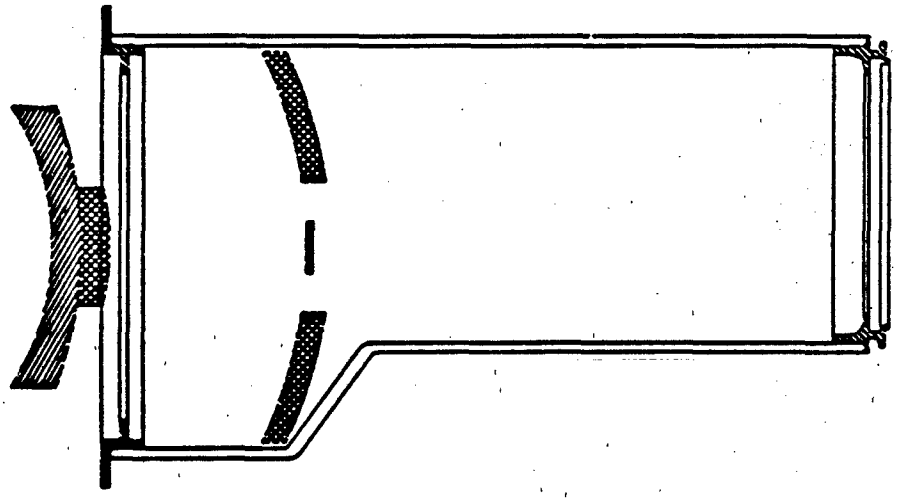

b) With Modified Receiver Housing

Figure 6.1 Installation of Gabor-Cassegrain Telescope in Receiver Housing

almost three 10 cm cubes.

In the Gabor-Cassegrain, the narrow-band filter can be installed within the structure of the folded telescope as shown in Figure 6.2. The filter is fabricated in a number of sections, perhaps six or eight and supported by a spider structure behind the refractive element of the hybrid. The individual sections are pivoted about their outer edges as shown in the figure. One advantage of this approach is that the sizes of the individual segments make fabrication of the filter somewhat easier. It should also be noted that heating elements can be incorporated in the spider support structure to provide thermal control of the filter. Detailed analyses have not been completed on the variation of the ray angles which pass through the filter when mounted at the optimum angle. However, estimates of the angles in the sagittal plane indicate that the angle variations are less than those encountered in the present system, where the angle spectrum is multiplied by the magnification of the afocal telescope. An isometric drawing of the Gabor-Cassegrain telescope is given in Figure 6.3. The isometric illustrates a six segment filter with one segment in an open condition. Figure 6.3 is an isometric of the hybrid telescope installed in a modified receiver housing.

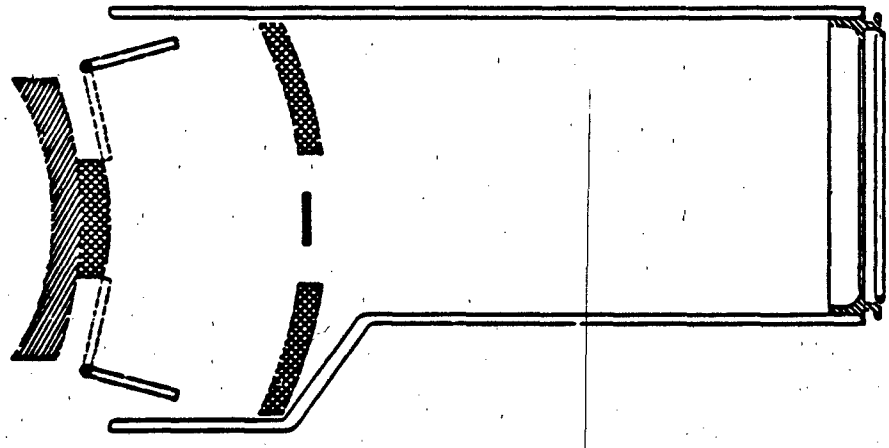

Figure 6.2 Gabor-Cassegrain Telescope with Spider and Removable Filter

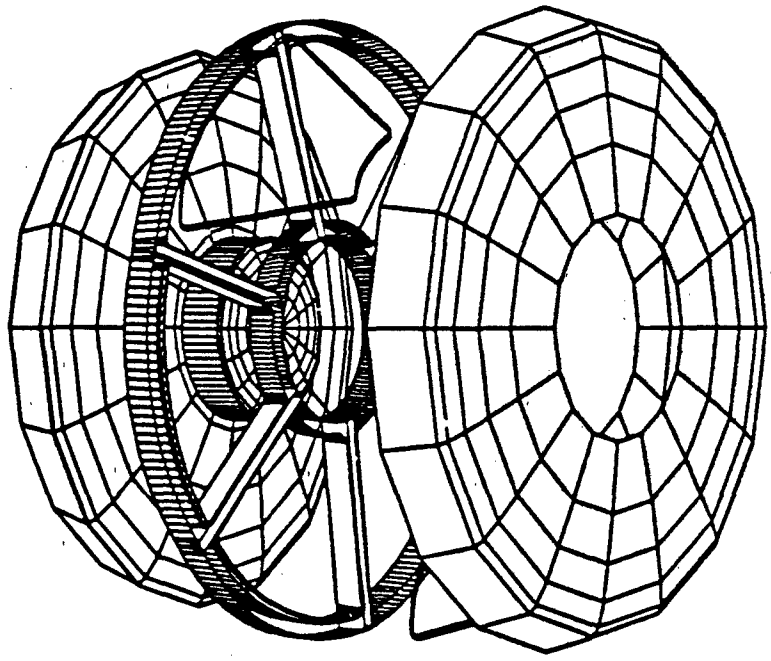

Figure 6.3 Isometric of Gabor-Cassegrain Telescope

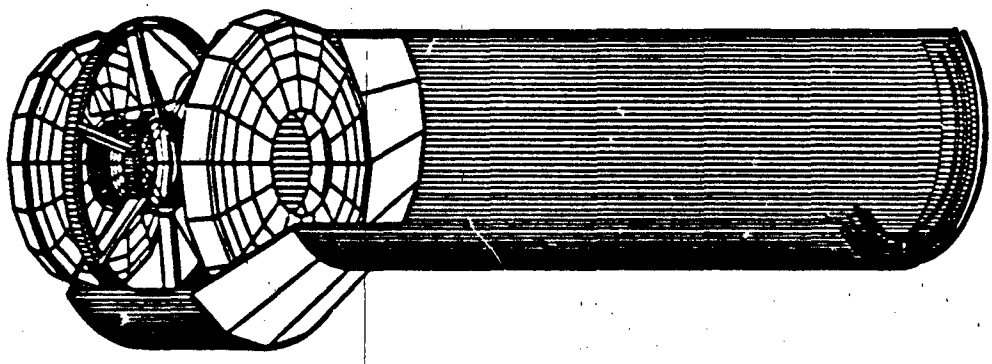

Figure 6.4 Gabor-Cassegrain Telescope and Filter Spider in Modified Housing

In summary, a relatively minor modification of the receiver housing will accommodate the hybrid Gabor-Cassegrain telescope which will save about 2,800 cm^3 of critical volume. The optical efficiency of the Gabor-Cassegrain exceeds that of the present refractive afocal and the image quality is sufficient to meet presently defined requirements for the identified missions.

7.0 CONCLUSIONS AND RECOMMENDATIONS

The recommended receiver consists of three subsystems:

1. Gabor-Cassegrain Telescope for low volume and weight and for compatibility with a segmented input filter,
2. Dual-Mode Digicon Detector for time-resolved search and high resolution identification of multiple target types,
3. Receiver Electronics to control the dual-mode Digicon and process the electronic signals in two separate modes.

The risks and recommendations for each subsystem are discussed in the following paragraphs.

The feasibility of the Gabor-Cassegrain telescope itself is well established. Additional design effort may be able to reduce further the aberrations and the corresponding image spot sizes, which are marginal for the very small targets, but are unnecessary for the two main targets of interest. The feasibility of using the segmented filter concept with the Gabor-Cassegrain telescope has not been established. A preliminary estimate of the ray angles in the sagittal plane indicates that the variation in angle is less than in the optical system of the present receiver. Additional analyses to evaluate the angles of all representative rays is needed. Furthermore, the results of this analysis should be compared with the angular performance of both the present filter and the filter upgrade which is presently being developed under contract with the Navy.

In addition to the feasibility of the angular acceptance of the segmented filter within the Gabor-Cassegrain telescope, there is an engineering issue concerned with the ability to fabricate and integrate a spider to support the filter, which is also capable of providing temperature control to the filter. Furthermore, the mechanical design of the spider and manipulators for the segmented filter may be quite difficult because of the confined space.

For the dual-mode Digicon, the only issue of feasibility is the ability to generate a high-quality electron image through the gating grid, which also provides for the high fields to enhance the quantum efficiency of the photocathode. The grid forms an equipotential surface which is

a plane located near the photocathode. Even though the separation is less than one millimeter, the equipotential surface will distort the electric fields which are used to re-image the electrons at the anode of the Digicon. This issue will be addressed in the current program to develop the APD Digicon as an upgrade for the present receiver. Using one of the 18 mm digicon tubes with a gating grid and a phosphor screen, we will evaluate the ability to form a high-quality image in the presence of a gating grid.

With the exception of high-quality imaging with a gating grid, all the technical features of the dual-mode Digicon have been individually demonstrated in a number of separate projects. However, there are a number of developmental issues related to the integration of multiple components into a single tube and fabrication of these components in a manner which is compatible with overall tube fabrication procedures, especially the high-temperature bake which is required for high-performance photocathodes. A partial list includes:

1. Thermal stability of the APD
2. Mounting the APD to the header to be compatible with high temperature baking with no out-gassing
3. Thermal stability of the CCD
4. Mounting the CCD to the header to be compatible with high temperature baking with no out-gassing
5. Mounting the grid and maintaining proper separation for control of electric field strength across the full photocathode
6. Providing for the thermal contact at the high voltage end of the tube to cool the photocathode.

Items 1 and 2 will be addressed during the course of the present program to develop the APD Digicon as a receiver upgrade.

All the issues for the electronic subsystem of the receiver deal with development, packaging and power consumption. Major development issues are cross-talk between channels and electronic interference between functions such as control of the Digicon focus and gating potentials and processing of the electronic signals from the detector. Packaging issues include

the placement and isolation of the focus, gating, deflection and diode bias power supplies for the Digicon detector, analog amplifiers for the APD quad, high-speed digitizers for the time-resolved signals, clock drivers for the CCD, digitizers for the CCD images and interfaces with the other major subsystems. Power consumption is a concern for the high-speed digitizers. None of these issues have been addressed during this conceptual design effort.

In order to reduce the risk in the development of the dual-mode Digicon for the operational upgrade of the receiver, the following additional tasks are recommended.

1. Gabor-Cassegrain Telescope Subsystem
   - 1.1 Evaluate expected filter performance for all rays and for present and planned filter upgrade approaches
   - 1.2 Further evaluate design concepts for improved image resolution in off-axis operation

2. Dual-Mode Digicon Detector Subsystem
   - 2.1 Select candidate CCD's for the dual-mode Digicon and evaluate thermal stability under thermal bake cycles used in tube fabrication
   - 2.2 Develop techniques for mounting the CCD's which are compatible with bake temperatures and tube out-gassing requirements
   - 2.3 Investigate alternative photocathode concepts which do not require cooling to reduce dark current

3. Receiver Electronic Subsystem
   - 3.1 Complete a preliminary design for all Dual-Mode Digicon power supplies to include technical approach and an assessment of volume, weight and power requirements
   - 3.2 Complete a preliminary design of all signal processing electronics to include an assessment of volume, weight and power requirements
   - 3.3 Complete a preliminary design of the high-speed digitizers to include an

assessment of volume, weight and power requirements

3.4 Integrate and package the preliminary designs of the components into the receiver pod to assess the feasibility of packaging the receiver subsystem.

Completion of the above tasks will substantially reduce the technical risk for development of the dual-mode Digicon receiver. Evaluating some of the electronics subsystems in breadboard experiments will provide additional risk reduction.